

Intestinal epithelial cell autophagy deficiency suppresses inflammation-associated colon tumorigenesis

Hao Liu,^{1,2,4} Jun Lou,^{1,4} Yunlong Liu,¹ Zhen Liu,¹ Jiansheng Xie,^{1,2} Jiachun Sun,³ Hongming Pan,¹ and Weidong Han¹

¹Department of Medical Oncology, Sir Run Run Shaw Hospital, School of Medicine, Zhejiang University, 3# East Qingchun Road, Hangzhou, Zhejiang, China; ²Laboratory of Cancer Biology, Institute of Clinical Science, Sir Run Run Shaw Hospital, School of Medicine, Zhejiang University, Hangzhou, Zhejiang, China; ³The First Affiliated Hospital, College of Clinical Medicine of Henan University of Science and Technology, Luoyang, Henan, China

Colitis-associated cancer (CAC) is closely related to chronic inflammation, whose underlying molecular mechanism, however, has not been elaborated comprehensively. In the current study, an investigation was conducted on the role of autophagy in the initiation and progression of azoxymethane (AOM)/dextran sulfate sodium (DSS)-induced colon tumors, a mouse model for CAC in humans. Mice with the intestinal epithelial cell (IEC)-specific deletion of the autophagy-related gene 7 (*Atg7*) saw a significant decrease in tumor number, burden, and risk of high-grade dysplasia. The autophagy deficiency of IECs resulted in the accumulation of T cells, especially CD8⁺ T lymphocytes in colon lamina propria. Furthermore, it was found that autophagy protects against DSS-induced intestinal injury through maintaining epithelial barrier function and promoting the survival and proliferation of IECs. Mechanistically, autophagy in IECs enhanced the activation of epithelial STAT3/ERK to promote the survival and proliferation of colonic epithelial cells during the development of CAC. Therefore, the findings unveil the essential role of autophagy in activating the processes of colonic protection, regeneration, and tumorigenesis.

INTRODUCTION

As a most common cancer, colorectal cancer (CRC) has been experiencing an increase in its diagnosed incidence rate worldwide,¹ whose pathogenesis is complicated and includes mutations, inflammatory bowel disease (IBD), gut microbiota, and lifestyle factors.² Among these, inflammation is a critical driver for CRC initiation, progression, and metastasis.³ Patients with IBD, including Crohn's disease and ulcerative colitis, are more likely to develop colitis-associated cancer (CAC), a subtype of CRC.⁴ However, the precise mechanism of linking chronic inflammation to colorectal tumor formation remains unclear.

As a conserved cellular process of clearing misfolded proteins and damaged organelles, autophagy is critical for the maintenance of cell survival and homeostasis.⁵ Autophagy-related gene 7 (*Atg7*), an E1-like enzyme, is of importance for the conjugation of Atg12, the lipidation of LC3, and the formation of autophagosome.⁶ Intestinal epithelial cells (IECs) are predominant components in the gastroin-

testinal tract and the first line of defense against bacterial invasion.⁷ A number of studies have reported that many critical functions of IECs are regulated by autophagy, which is implicated in the alteration of granule structure and the antimicrobial peptide secretion of goblet and Paneth cells under stress conditions.^{8–11} Epithelial autophagy has also been shown to recognize and degrade intracellular pathogens like *Salmonella* and *Citrobacter rodentium* infection, as autophagy deficiency in IECs led to enhanced susceptibility and inflammation.^{12,13} Moreover, autophagy in IECs protects against colitis via the maintenance of normal gut microflora and the secretion of mucus.¹⁴ In addition, epithelial autophagy controls chronic colitis by reducing tumor necrosis factor alpha (TNF α)-induced apoptosis.¹⁵

In tumorigenesis, autophagy is complex and context-dependent. Studies have shown that most patients with CRC and CRC cell lines experienced an increase in the expression of autophagy-associated proteins.^{16,17} Besides, a small number of patients with CRC were reported to have a lower expression of autophagic protein and impairment of autophagy.^{18,19} In the context of *Apc* conditional knockout mice, Lévy and colleagues²⁰ showed that inactivating *Atg7* in IECs inhibited tumor growth through a microbiome-induced immune response. In addition, *Atg7* deficiency led to a stress response accompanied by metabolic defects, AMPK activation and cell-cycle arrest mediated by p53 in tumor cells. Lucas and colleagues²¹ revealed that the inhibition of autophagy in IECs suppressed colonic tumorigenesis in *Apc*^{min/+} mice under normal circumstances but promoted Colibactin-producing *Escherichia coli*-induced colorectal carcinogenesis through increasing DNA damage and cell proliferation. Sakitani and colleagues demonstrated that the suppression of autophagy in colon cancer cells leads to a decrease in tumor size via promoting

Received 12 May 2021; accepted 17 February 2022;
<https://doi.org/10.1016/j.omtn.2022.02.012>

⁴These authors contributed equally

Correspondence: Weidong Han, Sir Run Run Shaw Hospital, School of Medicine, Zhejiang University, 3# East Qingchun Road, Hangzhou, Zhejiang 310016, China.
E-mail: hanwd@zju.edu.cn

Correspondence: Hongming Pan, Sir Run Run Shaw Hospital, School of Medicine, Zhejiang University, 3# East Qingchun Road, Hangzhou, Zhejiang 310016, China.
E-mail: panhongming@zju.edu.cn



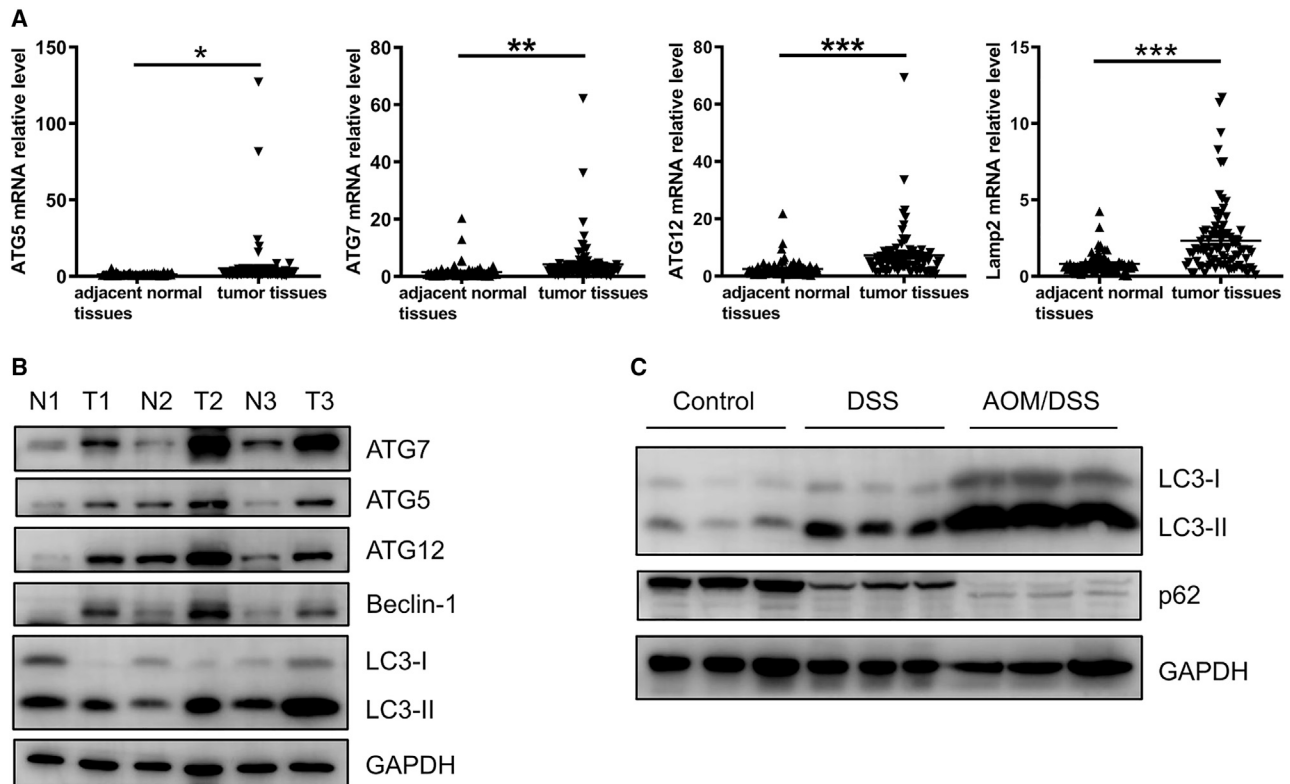


Figure 1. Autophagy is activated in tumor tissues of CRC patients and AOM/DSS-induced mice colon tumors

(A) The mRNA levels of autophagy-related genes in tumor tissues and paired adjacent normal tissues from 86 CRC patients were measured using real-time PCR. (B) Western blot analysis of autophagy-related proteins in tumor tissues (T) and paired adjacent normal tissues (N) of CRC patients ($n = 3$). (C) Western blot analysis of autophagy-related proteins in mice tumors and inflamed tissues. Data are represented as mean \pm SEM, * $p < 0.05$; ** $p < 0.01$; *** $p < 0.001$; according to the paired two-tailed, Student's *t* test.

p53 and endoplasmic reticulum stress-induced apoptosis.²² However, CAC is different from *Apc*-driven colon cancer in the initiation, promotion, and progression of tumorigenesis.^{23,24} Many animal models provide evidence that a variety of cytokines, chemokines, growth factors, and their receptors, as well as reactive oxygen species play a critical role in CAC.²⁵ Particularly, the oxidative injury that causes general DNA damage results in cancer initiation. Up to now, autophagy still plays an unclear role during CAC.

Herein, the role of autophagy in the carcinogenesis of a CAC mouse model following azoxymethane (AOM) and dextran sulfate sodium (DSS) administration was investigated. IEC-specific *Atg7* knockout mice were generated. It was demonstrated that autophagy could protect against DSS-induced epithelial damage and promote tumorigenesis. Mechanistically, autophagy enhanced the activation of epithelial STAT3/ERK to promote the survival and proliferation of colonic epithelial cells during the development of CAC.

RESULTS

Activation of autophagy in human CRC and murine CAC

First, the mRNA levels of various autophagy genes were analyzed by quantitative real-time PCR in tumors and the paired adjacent normal

tissues of patients with CRC. The expression levels of *ATG5*, *ATG7*, *ATG12*, and *Lamp2* mRNA increased markedly in the tumor tissues of 86 patients with CRC compared with those in adjacent normal tissues (Figure 1A), which were also reported in a previous study.¹⁹ Next, whether autophagy is activated in CRC patients was explored by analyzing LC3-I and LC3-II levels. It was observed that the level of LC3-II suggesting autophagy activation increased in tumors than in surrounding normal tissues (Figure 1B). Besides, other autophagy proteins, such as *ATG5*, *ATG7*, *ATG12*, and *Beclin1*, also saw an increase in tumors (Figure 1B). Finally, an AOM/DSS murine model was used for examining the expression levels of autophagy proteins in tumor initiation and promotion. Levels of LC3-II were significantly higher in tumors and inflamed tissues than in control specimens, while those of p62 degraded by functional autophagy decreased (Figure 1C). Therefore, these results demonstrate that autophagy is induced in the initiation and progression of colon cancer.

IECs *Atg7* deletion protects against AOM/DSS-induced colorectal tumorigenesis

Vil-cre⁺Atg7^{fl/fl} (hereafter referred to as *Atg7^{AIEC}*), and *Vil-cre⁻Atg7^{fl/fl}* mice (hereafter referred to as *Atg7^{fl/fl}*) models were established to analyze the role of autophagy in inflammation-related tumorigenesis.

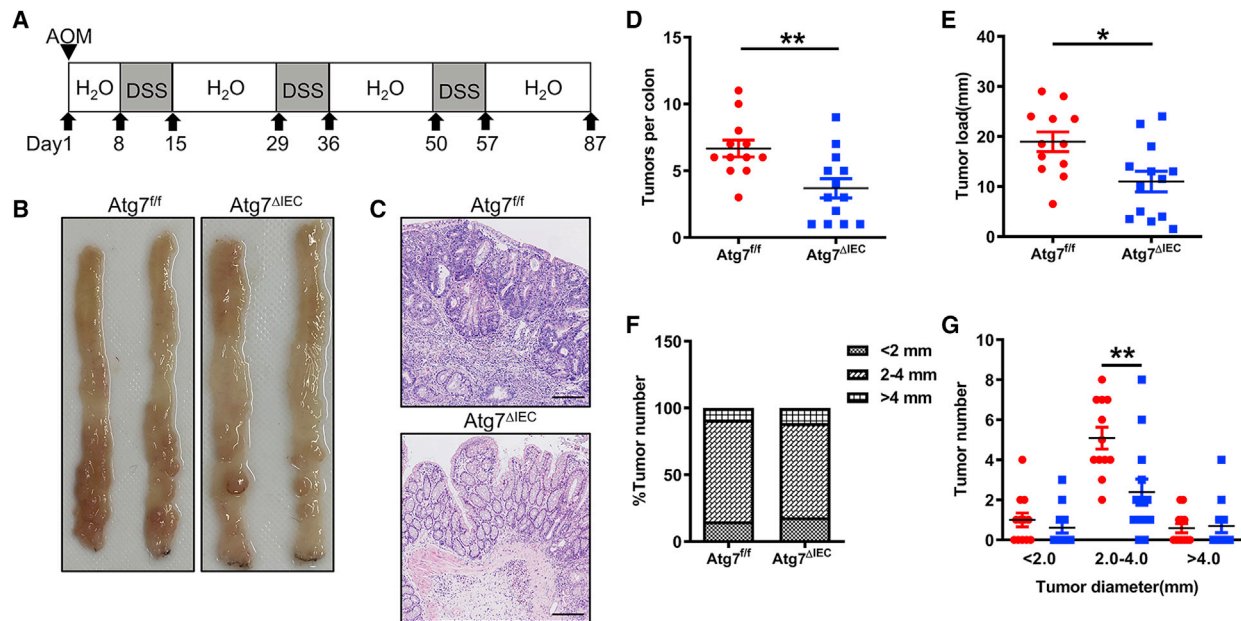


Figure 2. IECs *Atg7* deletion protects against AOM/DSS-induced colorectal tumorigenesis

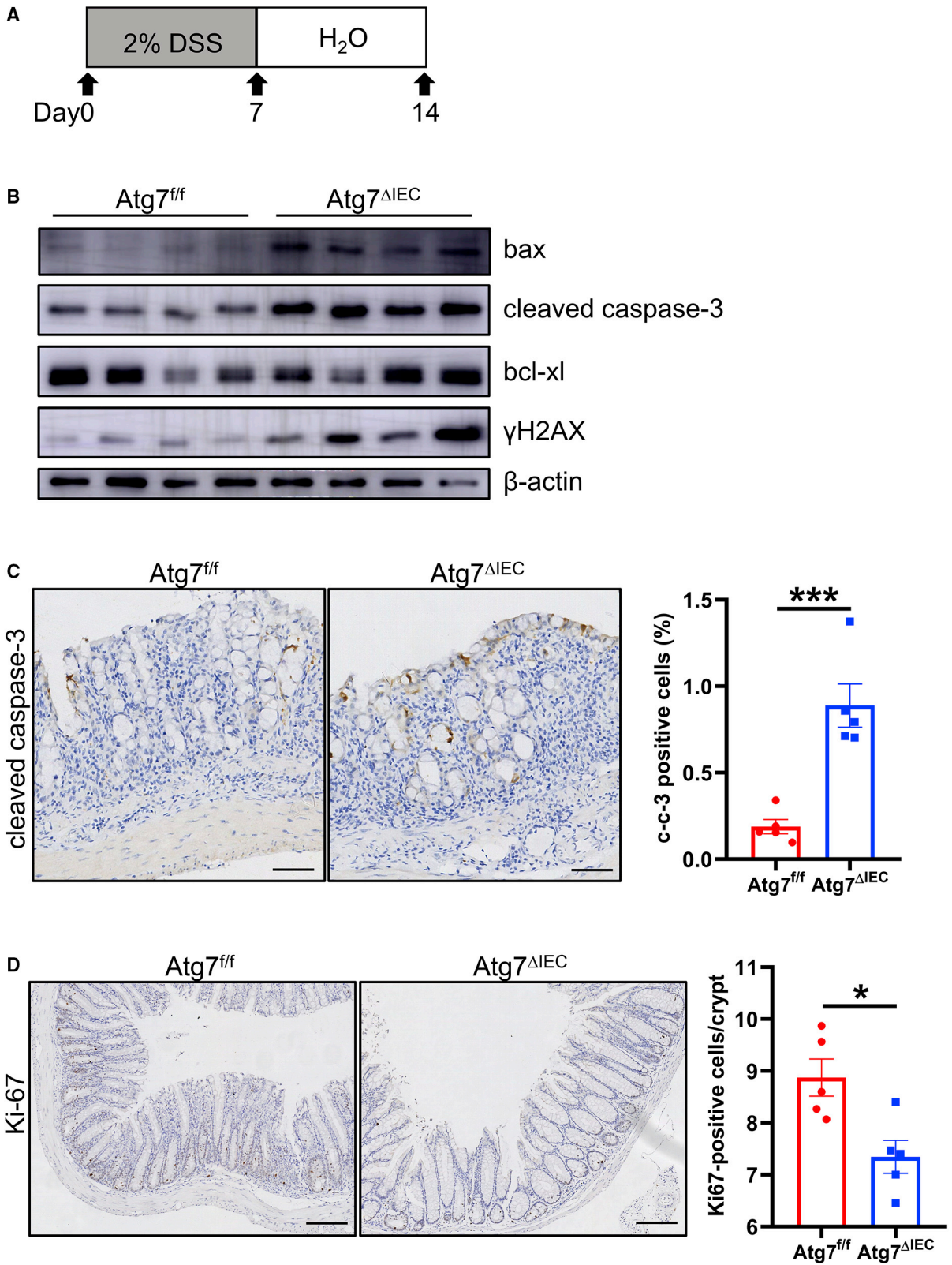
(A) Protocol of AOM/DSS-induced CAC in mice with analysis of intestinal tumors on day 87. (B) Gross morphology photographs of colon tissues from *Atg7^{fl/fl}* and *Atg7^{ΔIEC}* mice after exposure to AOM/DSS. (C) Representative H&E staining of colon slices from *Atg7^{fl/fl}* and *Atg7^{ΔIEC}* mice (bar, 200 μ m). (D–G) Tumor number (D), tumor load (E), tumor distribution (F), and classified tumor size (G) from the colon tissues of mice. (*Atg7^{fl/fl}* = 12, *Atg7^{ΔIEC}* = 13). Results are indicated as mean \pm SEM; **p* < 0.05, ***p* < 0.01, according to the unpaired two-tailed, Student's *t* test.

In the colorectal epithelium samples of *Atg7^{ΔIEC}* mice, *Atg7* expression was almost abolished (Figure S1A). Next, the intestinal defects of *Atg7^{ΔIEC}* mice during the steady state were explored. No significant differences were shown in colonic histology between *Atg7^{fl/fl}* and *Atg7^{ΔIEC}* mice (Figure S1B). The proliferation of IECs determined by the staining of Ki-67 and the analysis of Cyclin B1 and D1 expression by real-time PCR, was also free from the influence of *Atg7* deletion (Figures S1C–S1E). The comparison of immunohistochemical staining for active caspase-3 showed no obvious differences in epithelial apoptosis (Figures S1F–S1G). Then, an established colitis-associated colorectal tumorigenesis model in which mice were intraperitoneally injected with AOM and then three cycles of DSS was used (Figure 2A). Both AOM/DSS-treated *Atg7^{fl/fl}* and *Atg7^{ΔIEC}* mice developed tumors that were found primarily in the distal colon (Figure 2B). Histological analysis revealed that *Atg7^{ΔIEC}* mice exhibited low-grade dysplasia, whereas *Atg7^{fl/fl}* mice demonstrated high-grade dysplasia and adenomas (Figure 2C). The results showed that *Atg7^{ΔIEC}* mice developed much fewer tumors (Figure 2D) (6.67 ± 2.18 versus 3.69 ± 2.59 , respectively). The tumor load representing the total diameters of all tumors in a specific mouse decreased significantly in *Atg7^{ΔIEC}* compared with *Atg7^{fl/fl}* mice (Figure 2E) (18.96 ± 6.82 versus 11 ± 7.43 , respectively). Then, tumors were divided into three types according to their diameters. Tumor size distribution was not different between *Atg7^{fl/fl}* and *Atg7^{ΔIEC}* mice (Figure 2F). Although average tumor size showed no difference (data were not shown), middle-size (2–4 mm) tumors significantly declined in *Atg7^{ΔIEC}* compared with *Atg7^{fl/fl}* mice (Figure 2G). These results demonstrated

that autophagy deficiency in IECs could inhibit colitis-associated tumorigenesis.

Autophagy promotes IEC survival and proliferation during early tumor development

Previous studies revealed that altered apoptosis and proliferation in the early phases of tumor promotion in CAC models may affect the incidence and load of tumors.^{26,27} Thus, attention was paid to these time points to investigate the molecular mechanism of promoting colorectal tumorigenesis by autophagy. To probe into whether autophagy deficiency renders IECs more susceptible to apoptosis in early tumor promotion, *Atg7^{fl/fl}* and *Atg7^{ΔIEC}* mice were treated with DSS for inducing acute colitis (Figure 3A). *Atg7^{ΔIEC}* mice demonstrated more severe intestinal injury with a greater loss of weight than *Atg7^{fl/fl}* mice (Figure S2A), which was consistent with previous studies.¹³ *Atg7^{ΔIEC}* mice also displayed more severe colitis symptoms, including rectal bleeding, and abundant diarrhea, leading to higher clinical scores (Figure S2B). The extent of colitis was determined by measuring colon length, and *Atg7^{ΔIEC}* mice were found to have significantly shorter colons compared with *Atg7^{fl/fl}* mice (Figure S2C) (6.11 ± 0.29 versus 5.71 ± 0.26 , respectively). Consistent with these observations, H&E staining showed that *Atg7^{ΔIEC}* mice exhibited crypt destruction, infiltration of inflammatory cells, and ulceration, as indicated by higher histological score (Figure S2D). Moreover, interleukin (IL)-6 and TNF- α serum levels experienced a marked increase in



(legend on next page)

DSS-treated *Atg7^{ΔIEC}* mice relative to those in *Atg7^{fl/fl}* mice (Figure S2E).

Immunoblot analysis was performed to analyze whether autophagy protects IECs from death in the condition of inflammation-induced DNA damage. The results showed that caspase-3 in isolated *Atg7*-deficient IECs was significantly activated compared with that from *Atg7^{fl/fl}* mice, resulting in an enhanced apoptotic response (Figure 3B). Meanwhile, *Atg7^{ΔIEC}* mice were found to have the induction of proapoptotic proteins bax, and γ H2AX, a marker of DNA damage (Figure 3B). However, the expression of bcl-xL was similar though this antiapoptotic protein was induced by AOM/DSS treatment.²⁸ Immunohistochemistry (IHC) staining for active caspase-3 further confirmed that *Atg7^{ΔIEC}* mice had more apoptotic epithelial cells after DSS challenge than *Atg7^{fl/fl}* mice (Figure 3C). Collectively, these results show that the induction of bax and DNA damage rather than bcl-xL may explain the increased rate of apoptosis found in DSS-treated *Atg7^{ΔIEC}* mice.

IHC staining was carried out for Ki-67 to examine whether autophagy regulated cellular proliferation during the stage of epithelial regeneration. The results showed that *Atg7^{ΔIEC}* mice had fewer Ki-67-positive proliferating cells per crypt (Figure 3D), indicating a decrease in the proliferation of colonic epithelial cells during the regeneration stage of colitis. Importantly, unchallenged *Atg7^{fl/fl}* mice were not intrinsically different from *Atg7^{ΔIEC}* mice in proliferation.

Overall, these results suggest that autophagy protects mice from injury induced by colitis by raising the survival and proliferation of colonic epithelial cells.

Autophagy deficiency destroys epithelial barrier function

Intestinal barrier dysfunctions resulted in microbiota invasion, stimulating innate immune cells and causing excessive inflammation, tissue damage, and cell death.^{29,30} Next, the role of autophagy in regulating epithelial barrier function was determined. The expression of occludin and E-cadherin as important molecules modulating tight junctions and adherens junctions saw a reduction in the epithelia from *Atg7^{ΔIEC}* mice on day 7, while that of Zonula occludens-1 (ZO-1) was comparable (Figure 4A). IHC staining confirmed that *Atg7*-deficient colons exhibited disrupted or discontinuous E-cadherin staining, indicating the destruction of an intact and functional intestinal barrier in *Atg7^{ΔIEC}* mice (Figure 4B).

The impairment of epithelial barriers causes the infiltration of innate immune cells. The abundance of innate immune cells was

determined by IHC with marker macrophages (CD68) and neutrophils (myeloperoxidase [MPO]). The colons of *Atg7^{ΔIEC}* mice with DSS-induced colitis were found to have significantly increased neutrophils and macrophages compared with those of *Atg7^{fl/fl}* mice (Figure 4C). Moreover, real-timeRT-PCR results revealed that the expression of inflammatory cytokines and enzymes, including IL-1 β , IL-6, cyclooxygenase-2, TNF- α , IL-23a, and inducible nitric oxide synthase, in colonic tissues from *Atg7^{ΔIEC}* mice was significantly elevated (Figure 4D). These findings demonstrated that impaired epithelial barrier integrity in *Atg7^{ΔIEC}* mice contributed to excessive inflammation.

Autophagy deficiency inhibits STAT3 and ERK activation to restrict tumorigenesis

Relevant pathways known to be of importance in colonic carcinogenesis were explored with an aim of further defining autophagy's mechanism of affecting tumorigenesis. Mitogen-activated protein kinase (MAPK) pathways and STAT3 are the main factors modulating survival and proliferation during the development of cancer.^{31,32} As revealed by the western blot analysis of colon tumor lysates, phosphorylated STAT3 (p-STAT3), phosphorylated ERK1/2 (p-ERK1/2), and their main substrates cyclinD1 exhibited a marked decrease in *Atg7^{ΔIEC}* mice (Figure 5A). Accordingly, the expression of a few STAT3 target genes involved in the survival and proliferation of cells also decreased in *Atg7^{ΔIEC}* tumor tissues (Figure 5B). In line with these findings, IHC analysis confirmed that *Atg7^{ΔIEC}* mice saw a significant decrease in p-STAT3 and cyclinD1-positive cells compared with *Atg7^{fl/fl}* littermates (Figure 5C). It is well known that the survival and proliferation of premalignant epithelial cells are important for CAC development. The above signaling pathways still play a critical role in this process. To this end, the effects of autophagy deficiency during tumor initiation were examined. A significant decrease was observed in p-STAT3 and p-ERK1/2 in IECs from *Atg7^{ΔIEC}* mice on day 7 after the beginning of DSS treatment (Figure 5D). Therefore, autophagy plays an important role in the activation of STAT3 and ERK in IECs during tumor initiation and growth.

The requirement for STAT3 mediating the impacts of autophagy *in vivo* was examined. Besides, STAT3 inhibitor stattic was injected into *Atg7^{fl/fl}* and *Atg7^{ΔIEC}* mice at the stage of DSS challenge (Figure S3A). Compared with vehicle treatment, stattic treatment significantly aggravated weight loss, clinical scores, and colon length shortening in not only *Atg7^{fl/fl}* but also *Atg7^{ΔIEC}* mice (Figures S3B–S3D). However, autophagy failed to play a protective role after stattic administration (Figures S3B–S3D). H&E staining revealed that stattic-treated *Atg7^{ΔIEC}* mice showed similar epithelial damage levels and immune cell infiltration into the colonic lamina propria

Figure 3. Autophagy promotes the survival and proliferation of IECs in the early stage of tumor formation in the CAC model

(A) Scheme for colitis induction. Gray color indicates the duration of DSS treatment. (B) Western blot analysis of cleaved caspase 3, bax, bcl-xL, and γ H2AX (ser139) in the isolated IEC fraction on day 7. (C) Representative cleaved caspase 3 staining of colonic sections and quantification on day 7 (bar, 100 μ m). Image Pro Plus 6.0 was used to quantify cleaved caspase-3 positive cells and score three fields per mouse ($n = 5$ per group). (D) IHC using the anti-Ki-67 antibody of colonic sections on day 14 (bar, 200 μ m). Ki-67-positive cells were counted, and 15 to 18 full-length crypts per mouse colon were scored ($n = 5$ per group). Data are represented as mean \pm SEM, * $p < 0.05$; *** $p < 0.001$, according to the paired two-tailed, Student's *t* test.

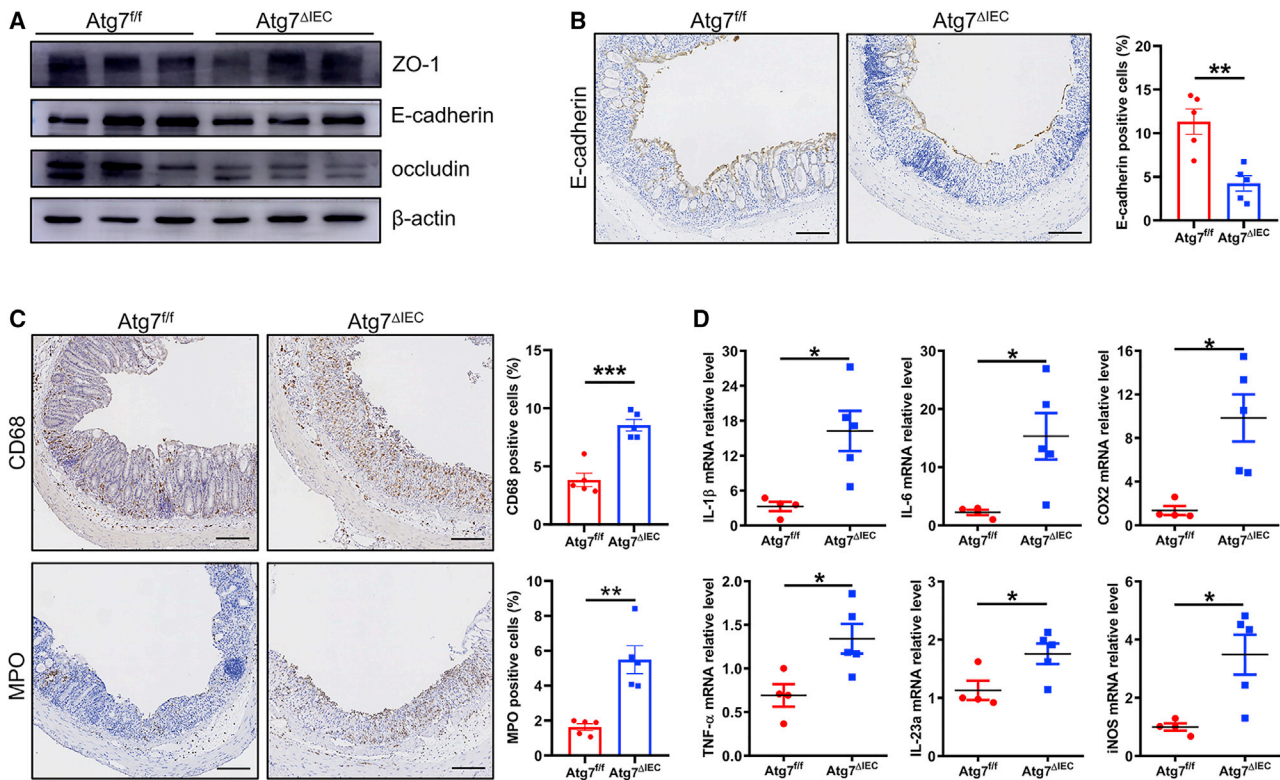


Figure 4. Autophagy deficiency disrupts epithelial barrier function

(A) Western blot detection for ZO-1, E-cadherin, and occludin expression in the IECs of *Atg7^{fl/fl}* and *Atg7^{ΔIEC}* mice on day 7 after DSS treatment. (B) IHC micrographs for E-cadherin expression in the colons of *Atg7^{fl/fl}* and *Atg7^{ΔIEC}* mice (bar, 200 μm). Quantification of E-cadherin staining by Image Pro Plus 6.0 (n = 5 per group) (C) IHC staining of MPO, and CD68 proteins in *Atg7^{fl/fl}* and *Atg7^{ΔIEC}* mice on day 7 (bar, 200 μm). Quantification of staining by Image Pro Plus 6.0 (n = 5 per group). (D) Relative mRNA levels of inflammatory cytokines and enzymes in the colons of *Atg7^{fl/fl}* and *Atg7^{ΔIEC}* mice (*Atg7^{fl/fl}* = 4, *Atg7^{ΔIEC}* = 5). Data are represented as mean ± SEM, *p < 0.05; **p < 0.01; ***p < 0.001, according to the paired or unpaired two-tailed, Student's t test.

compared with *Atg7^{fl/fl}* mice receiving static injection (Figures S3E and S3F). The results further indicate that autophagy promotes the survival and proliferation of IECs via the enhancement of STAT3 activation.

Autophagy deficiency in IECs enhances the immune response in colon tumors

Based on the decrease of tumor burden and multiplicity in *Atg7^{ΔIEC}* mice, the immune response in the tumor microenvironment during CAC was determined. First, the colon lamina propria cells in CAC models were separated to analyze the subsets of CD3⁺ T cells. Among the subsets of T cells, *Atg7^{ΔIEC}* mice displayed higher proportions of CD3⁺ T cells among CD45⁺ cells and CD8⁺ T cells among CD3⁺ cells, and decreased proportions of CD4⁺ T cells among CD3⁺ cells (Figure 6A). Given the changes of these immune populations, key immune response-regulating chemokines and cytokines were then measured. C-C ligand (CCL) chemokines CCL4 and CCL5, chemoattractants for innate immune cells,³³ increased significantly in *Atg7^{ΔIEC}* tumors (Figure 6B). Moreover, the tumors of *Atg7^{ΔIEC}* mice exhibited a significant increase in the levels of interferon-γ, a key cytokine involved in tumor cytotoxicity,³⁰

compared with those of *Atg7^{fl/fl}* mice. On the whole, these findings indicate that autophagy deficiency facilitates local antitumor immune response.

Failure of autophagy deficiency in myeloid cells to inhibit colitis-associated tumorigenesis

Atg7^{fl/fl} mice were crossed with *LysM-Cre* mice to assess the role played by autophagy in myeloid cells in colon tumorigenesis. Successful *Atg7* depletion in myeloid cells was confirmed by western blot (Figure S4A). *Atg7^{fl/fl}* and *Atg7^{ΔMYL}* mice were exposed to the AOM/DSS protocol to test whether decreased tumorigenesis was due to the epithelium-intrinsic effect. The results showed that *Atg7^{ΔMYL}* mice developed tumors comparable to *Atg7^{fl/fl}* mice (Figure S4B), and *Atg7* deletion had no effect on tumor number, load, size, and distribution (Figures S4C–S4F). Taken together, autophagy in epithelial cells rather than myeloid cells plays a critical role in promoting tumorigenesis in mice.

DISCUSSION

Chronic intestinal inflammation can favor CRC development, which is supported by the fact about an increase in the possibility of developing gastrointestinal neoplasia conferred by IBD.³⁴ Some studies

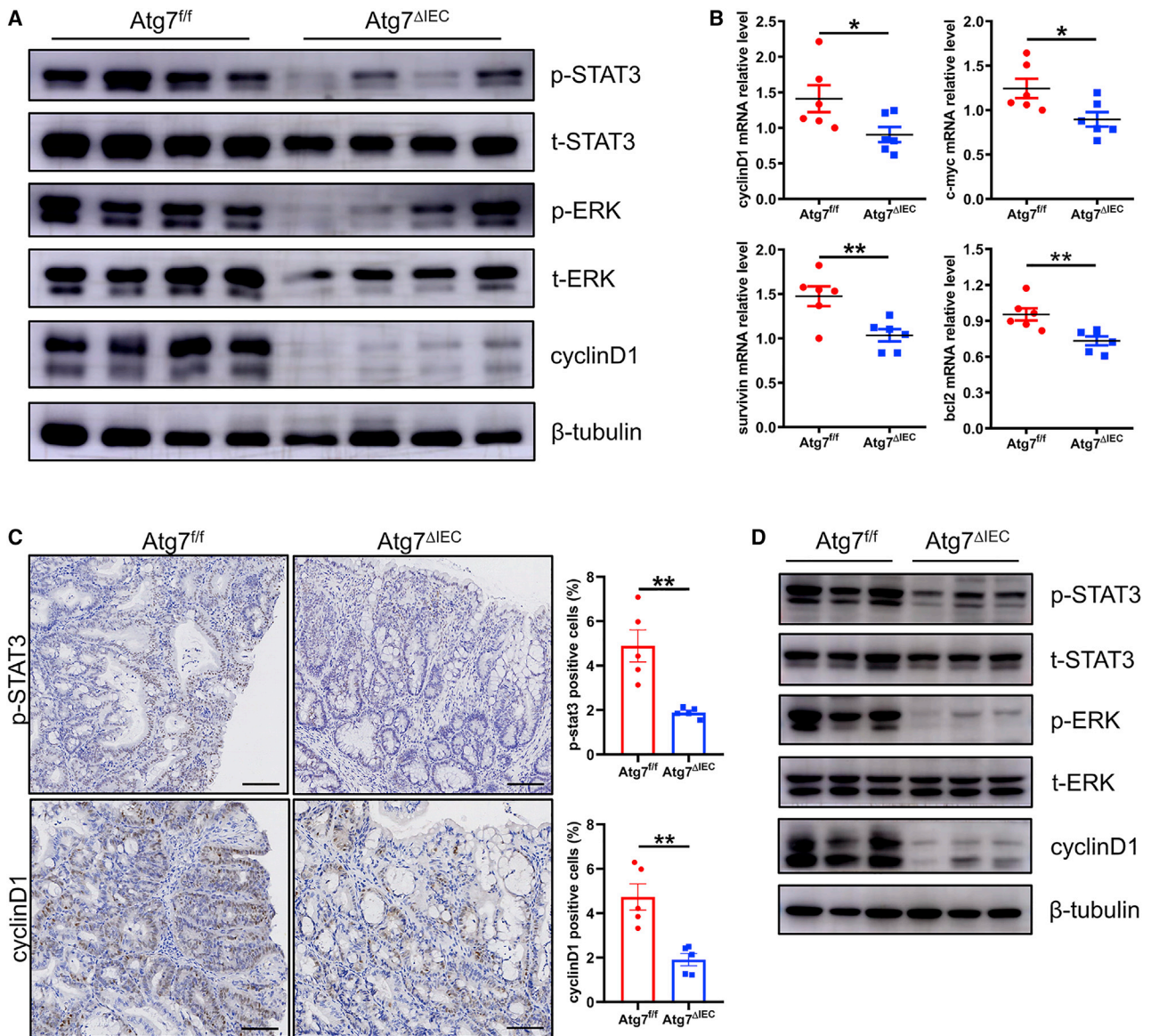


Figure 5. Atg7 deficiency inhibits the activation of STAT3/ERK signaling during acute colitis and CAC

(A) Tumor lysates from AOM/DSS-treated *Atg7^{fl/fl}* and *Atg7^{ΔIEC}* mice were analyzed by immunoblotting with the indicated antibodies. (B) Expression of STAT3 target genes in *Atg7^{fl/fl}* and *Atg7^{ΔIEC}* CAC tissues (n = 6 per group). (C) Images of p-STAT3 and cyclinD1 staining in CAC tumors from *Atg7^{fl/fl}* and *Atg7^{ΔIEC}* mice (bar, 100 μm). Quantification of staining by Image Pro Plus 6.0 (n = 5 per group) (D) IEC fraction from DSS-treated *Atg7^{fl/fl}* and *Atg7^{ΔIEC}* mice were analyzed by immunoblotting with the indicated antibodies. Data are represented as mean ± SEM, *p < 0.05; **p < 0.01, according to the paired two-tailed, Student's t test.

have reported that autophagy is implicated in the pathogenesis of human IBD.^{35,36} Nevertheless, it remains unknown whether autophagy plays a role in regulating the initiation and progression of CAC. In this paper, it was demonstrated that autophagy is upregulated in mouse colitis-associated tumors and human CRC. The IEC-specific knockout of *Atg7* greatly protects mice against tumorigenesis through regulating premalignant IEC survival and proliferation via the signaling of STAT3/ERK and accumulating T cells, especially CD8⁺ T lymphocytes in colon lamina propria during AOM/DSS-induced

CAC development. Targeting autophagy may be an effective strategy for treating and preventing CAC.

Prior research has reported that significantly fewer and smaller colonic tumors in *Apc^{+/-}Atg7^{-/-}* than *Apc^{+/-}* mice through enhancing antitumor responses maintained by the gut microbiota.¹⁹ The phenotype of the current study is in line with that of previous research, but the mechanism is not the same. Reports have shown that inflammatory mediators during CAC development support

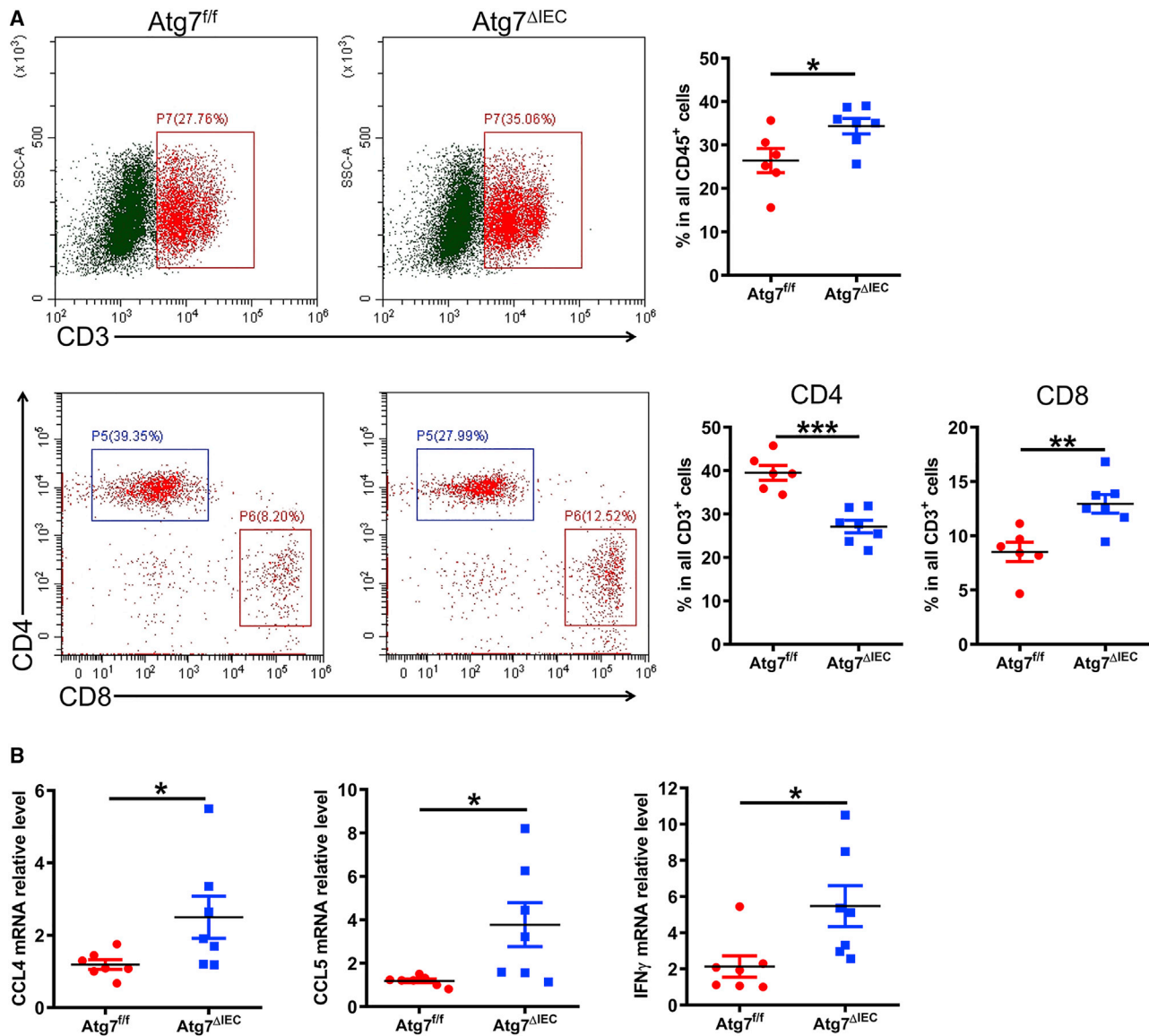


Figure 6. *Atg7* deficiency results in increased CD8⁺ T accumulation in colon lamina propria

(A) Representative fluorescence activated cell sorting results of T cell subsets in lamina propria and statistical results of CD3⁺ T, CD4⁺ T, CD8⁺ T cells (*Atg7^{fl/fl}* = 6, *Atg7^{ΔIEC}* = 7). (B) The mRNA levels of chemokines were assessed by real-time PCR from colonic tumors on day 87 after AOM/DSS treatment (n = 7 per group). Data are represented as mean \pm SEM, *p < 0.05; **p < 0.01; ***p < 0.001; according to the unpaired or paired two-tailed, Student's t test.

tumorigenesis initiation by oxidative stress-induced mutations and facilitate genetic instability.³⁷ Under continuous inflammatory conditions, *Atg7^{ΔIEC}* mice exhibited increased IEC apoptosis and decreased proliferation compared with *Atg7^{fl/fl}* ones. Moreover, *Atg7^{ΔIEC}* mice displayed an increased level of DNA damage, which was indicated by γ H2AX. Since proliferation associated with repair may be related to tumor growth, *Atg7* deletion during the induction of CAC led to a drastic reduction in tumor multiplicity and load. Intriguingly, myeloid-specific *Atg7* knockout had no phenotypes significantly differing from *Atg7^{fl/fl}* mice. Therefore, reduced IEC survival may

partially explain the increase of colitis but the reduction of colorectal adenomas in *Atg7^{ΔIEC}* mice.

Epithelial barrier integrity is important for the maintenance of intestinal homeostasis. An important component of epithelial barrier function is intercellular tight junctions, composed of ZO-1, occludin, and claudins.³⁸ Studies have found that several tight junction proteins, and E-cadherin, an adherens junction protein, show a reduction in both colitis and CRC.^{39,40} The data of the current study showed that autophagy deficiency destroyed intestinal barrier function during

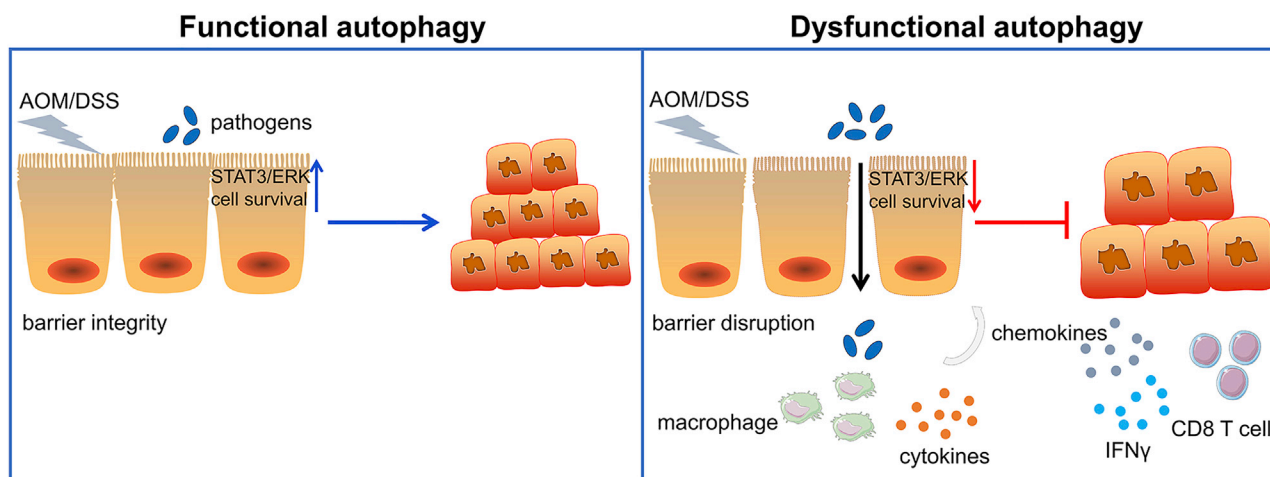


Figure 7. Proposed model for the role of autophagy in colorectal carcinogenesis

In response to AOM/DSS treatment, autophagy deficiency destroys epithelial barrier integrity to reduce the survival and proliferation of neoplastic epithelial cells by the inhibition of STAT3/ERK pathway, thus limiting colorectal carcinogenesis. Besides, autophagy dysfunction also induces an antitumor immune response by promoting the recruitment of T cells and the expression of key cytokines and chemokines to inhibit tumor growth. IFN, interferon.

experimental colitis, characterized by the decreased expression of E-cadherin and occludin compared with *Atg7^{fl/fl}* mice. However, future work needs to elaborate on autophagy's mechanism of regulating the cellular dynamics and localization of tight and adherent proteins.

Decreased premalignant IEC survival and proliferation found in *Atg7^{ΔIEC}* tumors raised the question about the underlying mechanism of autophagy. The STAT3 pathway has been involved in cell proliferation and oncogenic transformation during cancer pathogenesis in a variety of tissues.⁴¹ Bollrath and colleagues reported that STAT3 mediates the survival of IECs dependent on IL-6 and IL-11 and promotes proliferation by means of G1 and G2/M cell-cycle progression during colitis-associated tumorigenesis.⁴² MAPK pathways are major factors regulating cell growth and proliferation.⁴³ A study had reported that ATG proteins function as cellular scaffolds in the regulation of ERK phosphorylation.⁴⁴ In this study, *Atg7* deletion in IECs showed a decrease in the expression levels of p-STAT3 and p-ERK in CAC mouse models. The expression of proliferation-promoting genes like cyclin D1 and c-myc, and antiapoptosis genes like Mcl1 and Bcl2 are regulated by STAT3.⁴⁵ It was found that the expression levels of cyclin D1 and c-myc were downregulated in the tumors of *Atg7^{ΔIEC}* mice. During epithelial regeneration following DSS-induced injury, STAT3 and ERK phosphorylation also saw a drop in IECs from *Atg7^{ΔIEC}* mice. Thus, the results reveal that autophagy in IECs is important for both CAC initiation and progression through STAT3/ERK signaling activation and premalignant IEC survival and proliferation.

Apart from producing an epithelium autonomous effect, autophagy deficiency may also inhibit tumor growth by changing the immune response in colon tumors. The data of this study showed that the autophagy deficiency of IECs resulted in the accumulation of T cells, especially CD8⁺ T lymphocytes in colon lamina propria.

Besides, *Atg7^{ΔIEC}* mice exhibited increased macrophage and neutrophil infiltration in DSS-induced colitis. Overall, the changed tumor microenvironment without autophagy can restrict the growth of aberrant epithelial cells and tumor progression.

A previous study has identified that an *Atg5/Atg7*-independent autophagic pathway plays an important role in response to cytotoxic stressors.⁴⁶ In addition, it has been indicated that alternative autophagy can compensate for the functional role of conventional autophagy.⁴⁷ The current study failed to exclude the possibility that alternative autophagy in *Atg7* deletion in IECs is still activated by DSS or AOM/DSS. It is now necessary to conduct further studies to explore the functional role of alternative autophagy in CAC.

To sum up, the results demonstrate that autophagy deficiency protects against AOM/DSS-induced CAC through multiple mechanisms in colonic tumorigenesis and progression (Figure 7). In addition, autophagy deficiency destroys epithelial barrier integrity to promote the death of neoplastic epithelia in DSS-induced inflammation, and inhibits STAT3/ERK signaling activation, which is critical for the survival and proliferation of premalignant epithelial cells. Another axis promoted by autophagy deficiency is the antitumor immune response through promoting the recruitment of T cells and the expression of key cytokines and chemokines to inhibit tumor growth during the stage of CAC. Therefore, the findings of this study identify that epithelial autophagy might be a potential target to attenuate the progression of the intestinal tumors.

MATERIALS AND METHODS

Human samples

Eighty-six colon tumor tissues and matched non-tumorous colon tissues were obtained from Sir Run Run Shaw Hospital from 2018 to

2019. Thirty-five stage I-II and 51 stage III-IV patients with CRC were included. This study was approved by the Ethics Committee of Sir Run Run Shaw Hospital. Written informed consent was also obtained from all subjects before the study protocol. Tissue samples were collected and frozen in liquid nitrogen immediately after surgical resection.

Mice

Atg7 floxed mice (*Atg7^{fl/fl}* mice, RBRC02759)⁶ in a C57BL/6 background were purchased from the RIKEN Bio Resource Center. *Atg7^{ΔIEC}* mice were generated by crossing *Atg7^{fl/fl}* mice with *Villin-Cre* mice (The Jackson Laboratories). *Atg7^{ΔMYL}* mice were generated by crossing *Atg7^{fl/fl}* mice with *LysM-Cre* mice (The Jackson Laboratories). All the mice were subjected to a 12-h light/dark cycle in a pathogen-free animal facility, and were fed with standard rodent chow and water ad libitum. All animal experiments were approved by the Animal Care and Use Committee of Zhejiang University.

Induction of acute colitis and CAC

The acute colitis induced by DSS in mice was performed as reported previously.^{48,49} Briefly, male mice between 8 and 10 weeks old were treated with 2% DSS (molecular weight, 36,000–50,000; MP Biomedicals, Santa Ana, CA) in drinking water for 7 days, followed by regular drinking water for an additional 7 days. Body weight, diarrhea, and bloody stools were recorded daily.

CAC was induced in mice as previously described.^{44,45} Male mice between 8 and 10 weeks old were intraperitoneally injected with AOM (10 mg/kg, A5486; Sigma-Aldrich, St. Louis, MO). Seven days later, these mice were treated with 2% DSS in drinking water for 7 days, followed by regular drinking water for 2 weeks. This cycle was repeated twice, and all mice were killed at the indicated time points.

Histology staining and analysis

Tissue samples were fixed in 10% (v/v) formalin overnight, embedded in paraffin, sectioned, and stained with H&E. For IHC, paraffin sections were rehydrated with ethanol (Ante, Suzhou, China) after being deparaffinized with xylene (Aladdin, Shanghai, China). Endogenous peroxidase activity was inhibited by incubation of 3% H₂O₂ in methanol (Lingfeng, Shanghai, China), and slides were blocked with 10% BSA (Meilunbio, Dalian, China) for 1 h at room temperature. The slides were incubated overnight with primary antibodies at 4°C, followed by secondary antibodies for 30 min at room temperature. The following antibodies were used: Abcam (Ki-67, ab16667; CD68, ab125212; MPO, 208670), Cell Signaling Technology (cleaved caspase-3, 9664; γH2AX, 9718; E-cadherin, 3195; p-STAT3, 9145; cyclinD1, 2978).

RNA isolation and quantitative real-time PCR

Total RNAs from cells and tissues were extracted using RNAiso Plus reagent (9109; Takara, Tokyo, Japan). Reverse transcription was performed using the HiScript III first Strand cDNA Synthesis Kit (R312-02; Vazyme, Nanjing, China) according to manufacturer's instructions. The SYBR Green Master Mix (CW0659; Cwbiotech,

Beijing, China) was used to carry out real-time PCR. All the primers used for real-time RT-PCR were synthesized by Genaway (Shanghai, China). All the primer sequences used in this study are listed in Table S1.

Western blot and quantification

Total proteins from cells and tissues were extracted with RIPA lysis buffer (Meilunbio, Dalian, China) containing protease and phosphatase inhibitor cocktail (Bimake, Beijing, China). The concentration of protein was measured using BCA Protein Assay Kit (Genaway, Shanghai, China). Equal amounts of proteins (20 μg) were separated by 8% to 15% SDS-PAGE, then transferred to a PVDF membrane (Bio-Rad, Hercules, CA). The membrane was blocked with 5% non-fat milk in Tris-buffered saline plus Tween 20 (1%; Meilunbio, Dalian, China) solution, and incubated with the primary antibody overnight at 4°C, followed by incubation with appropriate horseradish peroxidase-conjugated secondary antibodies (Biotek, Hangzhou, China) for 1 h at room temperature. Signals were visualized using enhanced chemiluminescence (Amersham Imager 600; GE, Boston, MA). The antibodies obtained from different companies were as follows: Cell Signaling Technology (ATG7, 8558; ATG5, 12994; ATG12, 4180; Beclin-1, 3495; β-actin, 4970; Bax, 2772; Cleaved caspase-3, 9664; Bcl-xL, 2764; γH2AX, 9718; E-cadherin, 3195; p-STAT3, 9145; STAT3, 9139; ERK, 9102; p-ERK, 4370; cyclinD1, 2978), LC3 (Sigma, L7543), p62 (R&D, MAB8028), Thermo (ZO-1, 61–7300; Occludin, 71–1500), Huabio (β-tubulin, 0807-2; GAPDH, EM1101).

Isolation of IECs

IECs were isolated from the freshly dissected colon as previously described.⁴⁶ Briefly, colon tissues from mice were opened longitudinally, washed with ice-cold PBS, cut into 2-mm slices, and incubated in Hank's balanced salt solution (HBSS) (Sigma-Aldrich) containing 1.5 mM dithiothreitol (DTT) (Sigma-Aldrich) and 30 mM EDTA (Sigma-Aldrich) for 30 min at 4°C to remove mucus. Then, the mucosa was flushed in PBS and incubated in preheated HBSS with 30 mM EDTA and 2% fetal bovine serum (FBS) in a 37°C shaker for 30 min. The supernatant was gathered by centrifuging at 400 × g at 4°C for 10 min and washed twice with cold PBS.

Isolation of colonic lamina propria and flow cytometry analysis

The colonic lamina propria cells were isolated from the tissue remaining after the DTT and EDTA treatments. The tissues were cut into pieces and digested in RPMI media with 1.5 mg/mL collagenase, Type 4 (Sangon Biotech, Shanghai, China) and 2% FBS in a 37°C shaker for 1 h. The tissue debris was removed by a 40-μm cell strainer (Corning, Corning, NY) and cells were gathered by centrifugation (400 × g, 4°C, 10 min), washed twice with cold PBS, and stained with combinations of APC-conjugated anti-CD45 (Clone 30-F11; eBioscience, Thermo Fisher Scientific, Waltham, MA), PerCP/Cy 5.5-conjugated anti-CD3e (Clone 145-2C11; BD Biosciences, San Jose, CA), BV605-conjugated anti-CD4 (Clone RM4-5; BioLegend, San Diego, CA), and phycoerythrin-conjugated anti-CD8a (Clone 53-6.7; BioLegend) Abs, for analysis via an antirat/hamster BD

CompBeads™ (#552845; Becton Dickinson and Company, Franklin Lakes, NJ). The obtained profiles were analyzed by FlowJo software (Ashland, OR).

ELISA

The levels of IL-6 and TNF- α in serum were detected using ELISA kits (Invitrogen, Waltham, MA) according to the manufacturer's instructions. The results were calculated in pg/mL.

Stattic treatment

The STAT3 inhibitor stattic (MedChemExpress, Cat# HY-13818) was dissolved in vehicle (10% DMSO, 40% PEG300, 5% Tween-80, 45% saline) followed by intraperitoneal injection into mice treated with DSS at a dosage of 3.75 mg/kg once daily.⁵⁰ Control mice were only injected with vehicle.

Statistical analysis

GraphPad Prism software (GraphPad, San Diego, CA) was used for statistical analysis. Significant change between two groups were analyzed with Student's two-tailed t test. Data are presented as means \pm SEM. Statistical significance is represented by a p value of less than 0.05.

SUPPLEMENTAL INFORMATION

Supplemental information can be found online at <https://doi.org/10.1016/j.omtn.2022.02.012>.

ACKNOWLEDGMENTS

This work was supported by the National Natural Science Foundation of China (81902375, 81802842, 81772543, 81872500), the Ten Thousand Plan Youth Talent Support Program of Zhejiang Province (ZJWR0108009), and the Zhejiang Medical Innovative Discipline Construction Project-2016.

AUTHOR CONTRIBUTIONS

W.H. and H.P. conceived and designed the study. H.L., J.L., Y.L., Z.L., and J.X. performed the experiments. W.H. and H.L. analyzed the data and prepared the figures. W.H. and H.L. wrote the paper. J.S. modified the paper. All authors reviewed the manuscript, and the manuscript is approved by all authors for publication.

DECLARATION OF INTERESTS

The authors declare that they have no conflict of interest.

REFERENCES

1. Siegel, R.L., Miller, K.D., Goding Sauer, A., Fedewa, S.A., Butterly, L.F., Anderson, J.C., Cercek, A., Smith, R.A., and Jemal, A. (2020). Colorectal cancer statistics, 2020. *CA. Cancer J. Clin.* *70*, 145–164.
2. Kuipers, E.J., Grady, W.M., Lieberman, D., Seufferlein, T., Sung, J.J., Boelens, P.G., van de Velde, C.J., and Watanabe, T. (2015). Colorectal cancer. *Nat. Rev. Dis. Primers* *1*, 15065.
3. Rogler, G. (2014). Chronic ulcerative colitis and colorectal cancer. *Cancer Lett.* *345*, 235–241.
4. Fumery, M., Dulai, P.S., Gupta, S., Prokop, L.J., Ramamoorthy, S., Sandborn, W.J., and Singh, S. (2017). Incidence, risk factors, and outcomes of colorectal cancer in patients with Ulcerative Colitis with low-grade dysplasia: a systematic review and meta-analysis. *Clin. Gastroenterol. Hepatol.* *15*, 665–674.
5. Mizushima, N. (2018). A brief history of autophagy from cell biology to physiology and disease. *Nat. Cell Biol.* *20*, 521–527.
6. Komatsu, M., Waguri, S., Ueno, T., Iwata, J., Murata, S., Tanida, I., Ezaki, J., Mizushima, N., Ohsumi, Y., Uchiyama, Y., et al. (2005). Impairment of starvation-induced and constitutive autophagy in Atg7-deficient mice. *J. Cell Biol.* *169*, 425–434.
7. Benjamin, J.L., Sumpter, R., Jr., Levine, B., and Hooper, L.V. (2013). Intestinal epithelial autophagy is essential for host defense against invasive bacteria. *Cell Host Microbe* *13*, 723–734.
8. Adolph, T.E., Tomczak, M.F., Niederreiter, L., Ko, H.J., Böck, J., Martinez-Naves, E., Glickman, J.N., Tschurtschenthaler, M., Hartwig, J., Hosomi, S., et al. (2013). Paneth cells as a site of origin for intestinal inflammation. *Nature* *503*, 272–276.
9. Cadwell, K., Patel, K.K., Maloney, N.S., Liu, T.C., Ng, A.C.Y., Storer, C.E., Head, R.D., Xavier, R., Stappenbeck, T.S., and Virgin, H.W. (2010). Virus-plus-susceptibility gene interaction determines Crohn's disease gene Atg16L1 phenotypes in intestine. *Cell* *141*, 1135–1145.
10. Lassen, K.G., Kuballa, P., Conway, K.L., Patel, K.K., Becker, C.E., Peloquin, J.M., Villablanca, E.J., Norman, J.M., Liu, T.C., Heath, R.J., et al. (2014). Atg16L1 T300A variant decreases selective autophagy resulting in altered cytokine signaling and decreased antibacterial defense. *Proc. Natl. Acad. Sci. U S A* *111*, 7741–7746.
11. Patel, K.K., Miyoshi, H., Beatty, W.L., Head, R.D., Malvin, N.P., Cadwell, K., Guan, J.L., Saitoh, T., Akira, S., Seglen, P.O., et al. (2013). Autophagy proteins control goblet cell function by potentiating reactive oxygen species production. *EMBO J.* *32*, 3130–3144.
12. Conway, K.L., Kuballa, P., Song, J.H., Patel, K.K., Castoreno, A.B., Yilmaz, O.H., Jijon, H.B., Zhang, M., Aldrich, L.N., Villablanca, E.J., et al. (2013). Atg16L1 is required for autophagy in intestinal epithelial cells and protection of mice from Salmonella infection. *Gastroenterology* *145*, 1347–1357.
13. Inoue, J., Nishiumi, S., Fujishima, Y., Masuda, A., Shiomi, H., Yamamoto, K., Nishida, M., Azuma, T., and Yoshida, M. (2012). Autophagy in the intestinal epithelium regulates *Citrobacter rodentium* infection. *Arch. Biochem. Biophys.* *521*, 95–101.
14. Tsuboi, K., Nishitani, M., Takakura, A., Imai, Y., Komatsu, M., and Kawashima, H. (2015). Autophagy protects against colitis by the maintenance of normal gut microflora and secretion of mucus. *J. Biol. Chem.* *290*, 20511–20526.
15. Pott, J., Kabat, A.M., and Maloy, K.J. (2018). Intestinal epithelial cell autophagy is required to protect against TNF-induced apoptosis during chronic colitis in mice. *Cell Host Microbe* *23*, 191–202.e4.
16. Zheng, H.Y., Zhang, X.Y., Wang, X.F., and Sun, B.C. (2012). Autophagy enhances the aggressiveness of human colorectal cancer cells and their ability to adapt to apoptotic stimulus. *Cancer Biol. Med.* *9*, 105–110.
17. Jo, Y.K., Kim, S.C., Park, I.J., Park, S.J., Jin, D.H., Hong, S.W., Cho, D.H., and Kim, J.C. (2012). Increased expression of ATG10 in colorectal cancer is associated with Lymphovascular invasion and lymph node metastasis. *PLoS One* *7*, e52705.
18. Chen, Z., Li, Y., Zhang, C., Yi, H., Wu, C., Wang, J., Liu, Y., Tan, J., and Wen, J. (2013). Downregulation of Beclin1 and impairment of autophagy in a small population of colorectal cancer. *Dig. Dis. Sci.* *58*, 2887–2894.
19. Cho, D.H., Jo, Y.K., Kim, S.C., Park, I.J., and Kim, J.C. (2012). Down-regulated expression of ATG5 in colorectal cancer. *Anticancer Res.* *32*, 4091–4096.
20. Lévy, J., Cacheux, W., Bara, M.A., L'Hermitte, A., Lepage, P., Fraudeau, M., Trentesaux, C., Lemarchand, J., Durand, A., Crain, A.M., et al. (2015). Intestinal inhibition of Atg7 prevents tumour initiation through a microbiome-influenced immune response and suppresses tumour growth. *Nat. Cell Biol.* *17*, 1062–1073.
21. Lucas, C., Salesse, L., Hoang, M.H.T., Bonnet, M., Sauvanet, P., Larabi, A., Godfraind, C., Gagnière, J., Pezet, D., Rosenstiel, P., et al. (2020). Autophagy of intestinal epithelial cells inhibits colorectal carcinogenesis induced by Colibactin-producing *Escherichia coli* in *ApcMin/+* mice. *Gastroenterology* *158*, 1373–1388.
22. Sakitani, K., Hirata, Y., Hikiba, Y., Hayakawa, Y., Ihara, S., Suzuki, H., Suzuki, N., Serizawa, T., Kinoshita, H., Sakamoto, K., et al. (2015). Inhibition of autophagy exerts anti-colon cancer effects via apoptosis induced by p53 activation and ER stress. *BMC Cancer* *15*, 795.

23. Terzic, J., Karin, E., and Karin, M. (2010). Inflammation and colon cancer. *Gastroenterology* *138*, 2101–2114.
24. Ullman, T.A., and Itzkowitz, S.H. (2011). Intestinal inflammation and cancer. *Gastroenterology* *140*, 1807–1816.e1.
25. Danese, S., and Mantovani, A. (2010). Inflammatory bowel disease and intestinal cancer: a paradigm of the Yin-Yang interplay between inflammation and cancer. *Oncogene* *29*, 3313–3323.
26. Sheng, Y.H., Wong, K.Y., Seim, I., Wang, R., He, Y., Wu, A., Patrick, M., Lourie, R., Schreiber, V., Giri, R., et al. (2019). MUC13 promotes the development of colitis-associated colorectal tumors via β -catenin activity. *Oncogene* *38*, 7294–7310.
27. Liu, Z.Y., Zheng, M., Li, Y.M., Fan, X.Y., Wang, J.C., Li, Z.C., Yang, H.J., Yu, J.M., Cui, J., Jiang, J.L., et al. (2019). RIP3 promotes colitis-associated colorectal cancer by controlling tumor cell proliferation and CXCL1-induced immune suppression. *Theranostics* *9*, 3659–3673.
28. Greten, F.R., Eckmann, L., Greten, T.F., Park, J.M., Li, Z.W., Egan, L.J., Kagnoff, M.F., and Karin, M. (2004). IKK β links inflammation and tumorigenesis in a mouse model of colitis-associated cancer. *Cell* *118*, 285–296.
29. Luissint, A.C., Parkos, C.A., and Nusrat, A. (2016). Inflammation and the intestinal barrier: leukocyte–epithelial cell interactions, cell junction remodeling, and mucosal repair. *Gastroenterology* *151*, 616–632.
30. Wells, J.M., Brummer, R.J., Derrien, M., MacDonald, T.T., Troost, F., Cani, P.D., Theodorou, V., Dekker, J., Méheust, A., De Vos, W.M., et al. (2017). Homeostasis of the gut barrier and potential biomarkers. *Am. J. Physiol. Gastrointest. Liver Physiol.* *312*, G171–G193.
31. Setia, S., Nehru, B., and Sanyal, S.N. (2014). Upregulation of MAPK/Erk and PI3K/Akt pathways in ulcerative colitis-associated colon cancer. *Biomed. Pharmacother.* *68*, 1023–1029.
32. Grivennikov, S., Karin, E., Terzic, J., Mucida, D., Yu, G.Y., Vallabhapurapu, S., Scheller, J., Rose-John, S., Cheroutre, H., Eckmann, L., et al. (2009). IL-6 and Stat3 are required for survival of intestinal epithelial cells and development of colitis-associated cancer. *Cancer Cell* *15*, 103–113.
33. Spranger, S., Bao, R., and Gajewski, T.F. (2015). Melanoma-intrinsic β -catenin signaling prevents anti-tumour immunity. *Nature* *523*, 231–235.
34. Waldner, M.J., Rath, T., Schürmann, S., Bojarski, C., and Atreya, R. (2017). Imaging of mucosal inflammation: current technological developments, clinical implications, and future perspectives. *Front. Immunol.* *8*, 1256.
35. Lassen, K.G., and Xavier, R.J. (2017). Genetic control of autophagy underlies pathogenesis of inflammatory bowel disease. *Mucosal Immunol.* *10*, 589–597.
36. Wu, Y., Yao, J., Xie, J., Liu, Z., Zhou, Y., Pan, H., and Han, W. (2018). The role of autophagy in colitis-associated colorectal cancer. *Signal Transduct. Target. Ther.* *3*, 31.
37. Waldner, M.J., and Neurath, M.F. (2014). Mechanisms of immune signaling in colitis-associated cancer. *Cell Mol. Gastroenterol. Hepatol.* *1*, 6–16.
38. Turner, J.R. (2009). Intestinal mucosal barrier function in health and disease. *Nat. Rev. Immunol.* *9*, 799–809.
39. Liu, W.C., Chen, Y.Z., Golan, M.A., Annunziata, M.L., Du, J., Dougherty, U., Kong, J., Musch, M., Huang, Y., Pekow, J., et al. (2013). Intestinal epithelial vitamin D receptor signaling inhibits experimental colitis. *J. Clin. Invest.* *123*, 3983–3996.
40. Rokavec, M., Öner, M.G., Li, H., Jackstadt, R., Jiang, L., Lodygin, D., Kaller, M., Horst, D., Ziegler, P., Schwitalla, S., et al. (2014). IL-6R/STAT3/miR-34a feedback loop promotes EMT-mediated colorectal cancer invasion and metastasis. *J. Clin. Invest.* *124*, 1853–1867.
41. Zhang, H.F., and Lai, R. (2014). STAT3 in cancer: friend or foe? *Cancers (Basel)* *6*, 1408–1440.
42. Bollrath, J., Pheese, T.J., von Burstin, V.A., Putoczki, T., Bennecke, M., Bateman, T., Nebelsiek, T., Lundgren-May, T., Canli, Ö., Schwitalla, S., et al. (2009). gp130-mediated Stat3 activation in enterocytes regulates cell survival and cell-cycle progression during colitis-associated tumorigenesis. *Cancer Cell* *15*, 91–102.
43. Dhillon, A.S., Hagan, S., Rath, O., and Kolch, W. (2007). MAP kinase signalling pathways in cancer. *Oncogene* *26*, 3279–3290.
44. Martinez-Lopez, N., Athonvarangkul, D., Mishall, P., Sahu, S., and Singh, R. (2013). Autophagy proteins regulate ERK phosphorylation. *Nat. Commun.* *4*, 2799.
45. Al Zaid Siddiquee, K., and Turkson, J. (2008). STAT3 as a target for inducing apoptosis in solid and hematological tumors. *Cell Res.* *18*, 254–267.
46. Nishida, Y., Arakawa, S., Fujitani, K., Yamaguchi, H., Mizuta, T., Kanaseki, T., Komatsu, M., Otsu, K., Tsujimoto, Y., and Shimizu, S. (2009). Discovery of Atg5/Atg7-independent alternative macroautophagy. *Nature* *461*, 654–658.
47. Ra, E.A., Lee, T.A., Won Kim, S., Park, A., Choi, H.J., Jang, I., Kang, S., Hee Cheon, J., Cho, J.W., Eun Lee, J., et al. (2016). TRIM31 promotes Atg5/Atg7-independent autophagy in intestinal cells. *Nat. Commun.* *7*, 1–15.
48. Kuai, Y., Liu, H., Liu, D., Liu, Y., Sun, Y., Xie, J., Sun, J., Fang, Y., Pan, H., and Han, W. (2020). An ultralow dose of the NADPH oxidase inhibitor diphenyleiodonium (DPI) is an economical and effective therapeutic agent for the treatment of colitis-associated colorectal cancer. *Theranostics* *10*, 6743–6757.
49. Yao, J., Xie, J., Xie, B., Li, Y., Jiang, L., Sui, X., Zhou, X., Pan, H., and Han, W. (2016). Therapeutic effect of hydroxychloroquine on colorectal carcinogenesis in experimental murine colitis. *Biochem. Pharmacol.* *115*, 51–63.
50. Li, C., Iness, A., Yoon, J., Grider, J.R., Murthy, K.S., Kellum, J.M., and Kummerle, J.F. (2015). Non-canonical STAT3 activation regulates excess TGF- β 1 and Collagen I expression in muscle of stricturing Crohn's disease. *J. Immunol.* *194*, 3422–3431.